

Anomalous versus non-homogeneous diffusion in the ligand-binding equilibrium: when size matters

Hédi Soula,^{1,2,*} Bertrand Caré,^{1,2} Guillaume Beslon,^{1,3} and Hugues Berry^{1,3,†}

¹*EPI Beagle, INRIA Rhône-Alpes, F-69603, Villeurbanne, France*

²*Université de Lyon, Inserm UMR1060, F-69621 Villeurbanne, France*

³*LIRIS, Université de Lyon, UMR 5205 CNRS-INSA, F-69621, Villeurbanne, France*

Measurements of protein motion in living cells and membranes consistently report transient anomalous subdiffusion which converges back to a Brownian motion with reduced diffusion constant at long times, after the subdiffusion regime. On the other hand, membranes are also non-homogeneous media in which Brownian motion may be locally slowed-down due to variations in lipid composition. Here, we investigate whether both situations lead to a similar behavior for the reversible ligand-binding reaction in 2d. We compare the (long-time) equilibrium properties obtained with transient anomalous diffusion to those obtained with slowed-down Brownian motion. We show that both processes increase the apparent affinity of the reaction. However, in the case of slowed-down Brownian motion, the affinity is maximal when the slowdown is restricted to a subregion of the available space. Hence, these two processes are different: size matters for slowed-down Brownian motion, not for transient anomalous subdiffusion.

PACS numbers: 87.15.Vv, 82.39.Rt, 87.15.R-, 87.16.dp

Cell membranes are heterogeneous collections of contiguous spatial domains with various length and time scales (e.g. lipid rafts, caveolae) [1], that spatially modulate the lateral diffusion of proteins [2]. This defines an non-homogeneous diffusion problem, with position-dependent diffusion constant [3]. On the other hand, numerous studies [4–6] have shown that the lateral diffusion of lipids, proteins and multimolecular assemblies in cells and membranes exhibit subdiffusive anomalous diffusion (whereby the mean squared displacement scales sublinearly with time, $\langle \mathbf{r}^2(t) \rangle \propto t^\alpha$ with $\alpha < 1$), a hallmark of diffusion obstruction by obstacles [7] and, more generally, heavy-tailed jump-time distributions [7, 8]. However, in the latter situation, the anomalous regime is usually only transient: at long times, the mean squared displacement crosses back to normal (Brownian) diffusion, with $\alpha = 1$ but a reduced apparent diffusion constant [6]. Such transient behaviors are for instance obtained when the density of obstructing obstacles is below the percolation threshold [9]. This asymptotically slowed-down Brownian regime could be considered a mesoscopic (homogenized) representation of the underlying microscopic anomalous subdiffusion. At first sight, both situations could thus be considered equivalent on long time scales. Regarding the biochemical reactions that take place in these media, the influence of both situations has been relatively unexplored. Some results are available for transient reactions with transient anomalous subdiffusion – for the first binding times [10] and for Michaelis-Menten enzyme reactions and substrate consumption [11]. For position-dependent diffusion, the results are even sparser [12].

Here, we question the validity of the approximation that slowed-down Brownian motion could account for transient anomalous diffusion at long times. We study

the equilibrium properties of a reversible reaction when diffusion is transiently anomalous due to obstacles (below the percolation threshold) or when normal space-dependent Brownian diffusion takes place. We consider the ubiquitous ligand-binding equilibrium



where L is the ligand, R its free receptor, and C the bound complex. Reversible reactions are expected to converge at long times to equilibrium, thus permitting the study of the influence of both anomalous diffusion and space-dependent diffusion not only on transient but also long-time equilibrium properties. Note that in classical conditions, the equilibrium of Eq.(1) is well known (assuming $L_0 \gg R_0$, where L_0 and R_0 are the initial concentrations in ligand and receptor, respectively): $C_{\text{eq}} = R_0 L_0 / (K_D + L_0)$. This defines so-called dose-response curves – the equilibrium amounts of C for increasing doses of ligand – with equilibrium constant $K_D = k_{\text{on}}/k_{\text{off}}$, a measure of efficiency of the reaction.

To simulate diffusion, we initially position L and R molecules (and possibly, obstacles) uniformly at random on a 800×800 2D square lattice with periodic boundaries. Each lattice site (i, j) is associated with a diffusion constant $D(i, j)$ (all molecules here have identical diffusion constants). $D(i, j) = 0$ if (i, j) contains an obstacle. At each time step δt , every molecule is allowed to leave its current location (i, j) with probability $j(i, j) = 2d\delta t / (\delta x)^2 D(i, j)$, where δx is the lattice spacing and d the dimension. The destination site is chosen uniformly at random from the 4 nearest neighbors $(i \pm 1, j \pm 1)$ and the molecule jumps to it, except if the destination site contains an obstacle, in which case the molecule remains in its initial location (i, j) . If the jump

of the molecule to its destination site results in the presence of a (L,R) couple on the same lattice site, a binding event may occurs, i.e. the (L,R) couple is replaced by a single C molecule at the site, with probability p_{on} . Finally, at each time step, every C molecule can unbind, i.e. the C molecule is replaced by a (L,R) couple at the same site, with probability p_{off} .

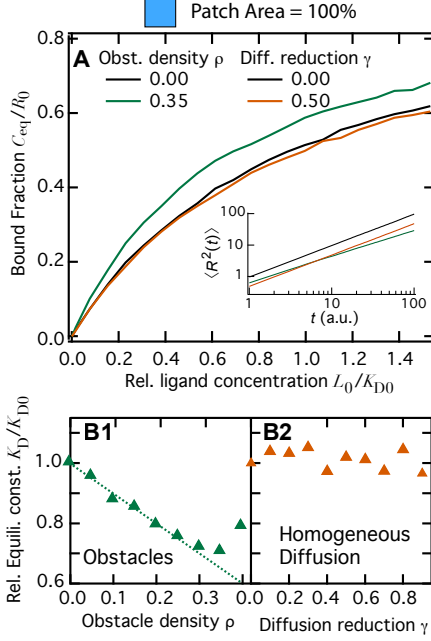


FIG. 1. Simulations of reaction eq.(1) in homogeneous conditions, $D(i, j) \equiv D, \forall i, j$. (A) Evolution of the bound fraction at equilibrium, C_{eq}/R_0 as a function of the relative ligand concentration L_0/K_{D0} , where K_{D0} is the value of K_D in the absence of obstacles and with reference diffusion constant D_0 . $(\rho, D) = (0.0, D_0)$ (black), $(0.0, D_0/2)$ (orange) or $(0.35, D_0)$ (green). The inset shows the initial regime of the corresponding mean-squared displacements (MSD). (B) Relative apparent equilibrium constant K_D/K_{D0} for $D = D_0$ and increasing ρ (B1) or no obstacles but increasing reduction of the diffusion, $\gamma = 1 - D/D_0$ (B2). The dashed line locates the diagonal $y = 1 - x$. Other parameters: $R_0 = 100$, $\delta t = \delta x = 1$, $p_{\text{on}} = 0.1$, $p_{\text{off}} = 10^{-3}$ and $D_0 = 1$, data are averages of 10 runs.

In a typical simulation, we start with R_0 R molecules and L_0 L, and run the simulation until the density of bound receptors C reaches a steady state, C_{eq} . As shown in Figure 1A we obtain the typical dose-response curves for the bound fraction at equilibrium C_{eq}/R_0 . From this we can retrieve for all situations the apparent equilibrium constant K_D . The control behavior – no obstacles and spatially constant diffusion, $D(i, j) = D_0$ (black curve) – is not changed when the diffusion constant is lowered over the whole space to $D_0/2$ (orange curve). Whereas the presence of obstacles strongly modifies the equilibrium (green curve, obstacle density $\rho = 0.35$), yielding lower K_D . Fig 1B displays K_D values for several obstacles density ρ (B1) and several diffusion constant reduc-

tions γ in the absence of obstacles (B2). Clearly, for these parameters the regime is reaction-limited: one order of magnitude span for D does not influence K_D . Far from the percolation threshold ($\rho = 0.41$), K_D decays linearly with obstacle density as $K_D/K_{D0} = 1 - \rho$. This is a simple effect of the excluded volume occupied by the obstacles since it disappears if the concentrations are computed on the basis of the accessible space $1 - \rho$, instead of the whole space (not shown). Therefore, hindered diffusion due to obstacles not only decreases the molecule mobility, it also increases the affinity ($\sim 1/K_D$) of the reaction.

The results presented so far are for homogeneous conditions, i.e. $D(i, j) \equiv D, \forall i, j$. But in living cells, the conditions are usually spatially non-homogeneous: spatial domains (lipid rafts, caveolae) give rise to position-dependent values of D ; obstacle density can also be spatially-variable, as major obstacles can be clustered. In the following, we addressed this situation by restricting the region of space where diffusion is modified to a central square patch of variable spatial extent. Diffusion is Brownian with coefficient D_0 outside the patch and reduced within the central patch either by the presence of obstacles or by imposing a reduced diffusion constant D_1 inside the patch.

Before addressing the ligand-binding equilibrium eq.(1) in these conditions, we first investigate diffusion effects alone. We used a central patch which surface area was 25% of the whole space and simulate the diffusion of diffusive non-reactive molecules until they reach equilibrium. Once equilibrium is reached, we perturb it by the addition of supplementary non-reactive molecules in the center of the patch and measure the characteristic time to reach a new equilibrium and the concentration of molecules inside the patch at this new equilibrium. Because reduced diffusion in the patch slows down the molecules, the characteristic time to converge back to equilibrium increases when diffusion is reduced in the patch, either because of obstacles (Fig. 2A1) or directly by decreasing D_1 (Fig. 2B1). Both cases are remarkably similar in that respect. The main differences occur for the equilibrium concentrations. With obstacles, the equilibrium concentration within the patch slightly decreases with increasing obstacle densities (Fig. 2A2). The results obtained for space-dependent Brownian conditions however strongly depart from the case with obstacles. We observe increasing accumulation of molecules within the patch when diffusion is decreased therein (Fig. 2B2). We emphasize here these are equilibrium conditions.

However surprising, this equilibrium effect can be directly predicted in our system. Let us consider the 1d case for simplicity, and a constant-by-part dependence of the diffusion constant $D(x) = D_1, \forall x \in [a, b]$ and $D(x) = D_0$ outside the patch $[a, b]$. Let us then consider a single molecule and let $\pi(x, t)$ its probability to

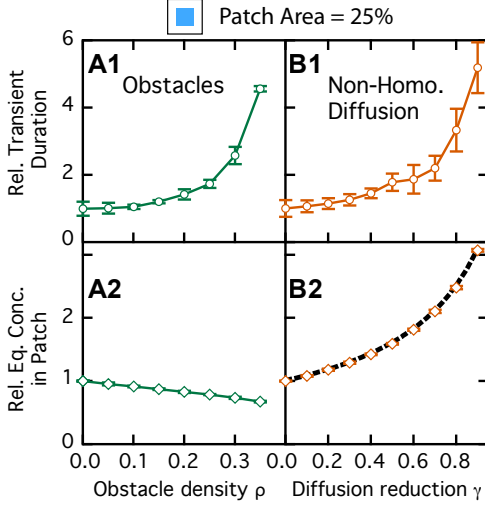


FIG. 2. Diffusion in non-homogeneous conditions. Non-reactive molecules diffuse with coefficient D_0 (no obstacles) outside of a central patch that contains obstacles at density ρ (A1-2) or in which the diffusion constant is reduced according to $D_1 = D_0(\gamma - 1)$ (no obstacles) (B1-2). The *top* row shows the characteristic time to reach equilibrium and the *bottom* one the molecule density at equilibrium in the patch. Data are normalized by the values obtained for $\rho = 0$ in the patch (A1-2) or when $\gamma = 0$ (B1-2). Full lines are guide to the eyes while the black dashed line in B2 shows the theoretical prediction eq. (7). All other parameters are as in Fig. 1.

be located at position x at time t [13]:

$$\pi(x, t + \delta t) = q(x)\pi(x, t) + \pi(x - \delta x, t)(1 - q(x - \delta x))/2 + \pi(x + \delta x, t)(1 - q(x + \delta x))/2 \quad (2)$$

where $q(x)$ is the probability not to jump at each time step and is defined, using the jump probability $j(x) = 2\delta t/(\delta x)^2 D(x)$ above, as $q(x) = 1 - j(x)$. Noting $g(x, t) = (1 - q(x))\pi(x, t)/2$ and developing $g(x \pm \delta x, t)$ in series of x , one obtains at order 2

$$\begin{aligned} \pi(x, t + \delta t) &= q(x)\pi(x, t) + 2g(x) + (\delta x)^2 \partial_{xx} g(x) \\ &= \pi(x, t) + (\delta x)^2 \partial_{xx} g(x, t) \end{aligned} \quad (3)$$

Dividing by δt and taking the limit $\delta t \rightarrow 0$, one gets

$$\partial_t \pi(x, t) = \partial_{xx} (D(x)\pi(x, t)) \quad (4)$$

where we used the expression of $j(x)$ above to define $D(x)$. Noting $u(x, \infty)$ the density of molecules at x at equilibrium, one expects from eq.(4)

$$D(x)u(x, \infty) = \mathcal{H}(D) \quad (5)$$

where $\mathcal{H}(D)$ is the spatial harmonic mean of the (space-dependent) diffusion function

$$\mathcal{H}(D) = \left[\int D^{-1}(x) dx \right]^{-1} \quad (6)$$

Now, using the constant-by-part function for $D(x)$ expressed above, this yields $u(x, \infty) = \mathcal{H}(D)/D_1 \forall x \in [a, b]$ and $u(x, \infty) = \mathcal{H}(D)/D_0$ outside. The equilibrium concentration inside the $[a, b]$ patch thus equals that found outside the patch multiplied by D_0/D_1 . Hence the larger the slowdown of the Brownian motion inside the patch, the larger the accumulation inside it at equilibrium explaining simulation results of Fig. 2B2. In the present 2d case, the total number of molecule in the patch N_{inside} relates to total number N_{total} , the surface fraction of the patch ϕ of the total surface S and the diffusion constant as:

$$N_{\text{inside}} = S\phi N_{\text{total}} \frac{\mathcal{H}(D)}{D_1}, \quad \mathcal{H}(D) = \left[\frac{\phi}{D_1} + \frac{1-\phi}{D_0} \right]^{-1} \quad (7)$$

Eq. (7) yields a very good prediction of the increase of equilibrium concentration of Fig. 2B2.

Such concentration changes are likely to modify the reaction in the non-homogeneous diffusion case. Using several sizes for the patch we computed the values of the apparent equilibrium constant K_D . With anomalous subdiffusion due to obstacles (Fig. 3A), the behavior reported in Fig. 1 is roughly conserved for all patch area fractions ϕ : K_D decreases linearly with the obstacle density ρ far from the percolation threshold then increases back close to it. The amplitude of this decay increases with the patch area (as the total space occupied by obstacles increases). Considering the behavior observed in spatially homogeneous conditions (Fig. 1B1), one expects, far from the percolation threshold, $K_D = K_{D0}(1-\phi) + K_{D0}(1-\rho)\phi$, yielding $K_D/K_{D0} = 1 - \rho\phi$. Indeed, we found that the latter is a very good approximation for the simulation results of Fig. 3A. Close to the percolation threshold, the increase of the first-collision time overcompensates by far the decrease of the re-collision times due to obstacles (not shown). As a result, the forward reaction rate k_{on} , and the apparent affinity, strongly decrease close to the threshold.

The situation is quite different for space-dependent diffusion (Fig. 3B). Whatever the patch size, we also observe that K_D decreases, but in this case, this is the result of the accumulation phenomenon reported above (Fig. 2B2). Moreover, in this case, K_D exhibits a non-monotonous dependency with respect to the area fraction ϕ , with a marked minimum. Hence, for a given value of diffusion reduction in the patch, $\gamma = 1 - D_1/D_0$, there exists an optimal value of the patch surface area that yields the highest affinity (Fig. 3B, inset). Assuming that reactions in the patch and outside are both reaction-limited and separable, one can estimate the extremum reached by C concentration using eq(7) for both R and L. From this, we derive a theoretical relation between γ and the optimal value of the patch surface, ϕ^* : $\gamma = 1 - \phi^*/(1 - \phi^*)$ (see Supplementary Material). The inset of Fig. 3B illustrates the good agreement with simu-

lation results. Therefore, non-homogeneous slowed-down Brownian systems exhibit a bonus to patchiness : the minimal value of K_D is obtained when the patch occupies a subset of the available space. This is in strong contrast with the equilibrium behavior obtained with transient anomalous subdiffusion above, where the affinity increases monotonously with the patch area fraction.

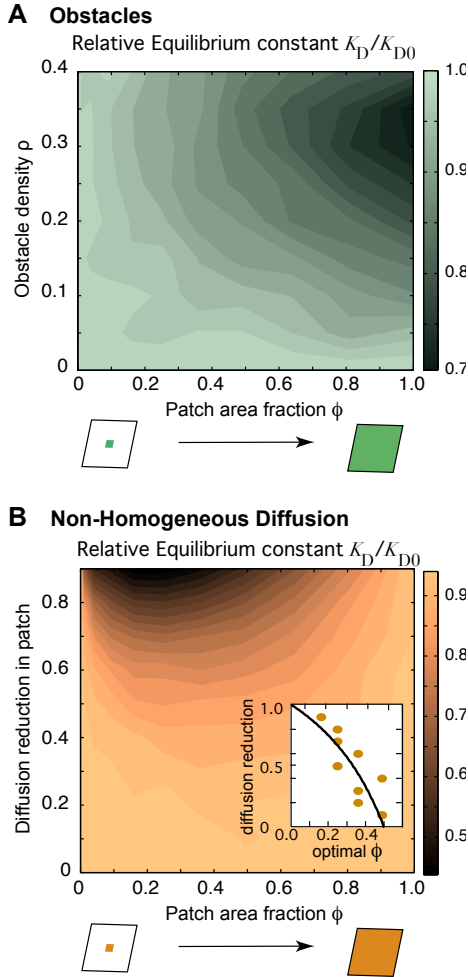


FIG. 3. Simulations of reaction eq.(1) in spatially non-homogeneous conditions. With transient anomalous subdiffusion (A) or reduced Brownian motion (B) inside a central patch, the apparent equilibrium constant K_D/K_{D0} is shown as a function of the area fraction occupied by the patch ϕ and the obstacle density ρ or the amount of diffusion reduction in the patch, $\gamma = 1 - D_1/D_0$. The inset in (B) locates the value of ϕ yielding maximal affinity (full circles) and the corresponding theoretical prediction (full line). All other parameters are as in Fig. 1.

In summary, we have shown that the equilibrium properties of the ligand-binding reaction eq.(1) differ when diffusion is slowed-down by anomalous subdiffusion due to obstacles or by a decrease of the diffusion constant due to, e.g., a change in lipid composition of the membrane. In both cases, slowing down the motion increases the ap-

parent affinity of the reaction. But in the former case, the increase of affinity is due to the decay of the accessible space, whereas in the latter, increased affinity is due to accumulation of molecules in the slowed-down zones. Moreover, in the case of anomalous subdiffusion, maximal affinity is obtained when the obstacles are spread all over the available space, whereas in the case of a space-dependent diffusion constant, maximal affinity is reached when the slowed-down region occupies only a restricted area. It is very tempting to remark that, in living cell membranes, slowed-down regions (rafts) show a very patchy distribution, whereas bulky obstacles seem less systematically clustered in limited regions. Controlling the spatial extension of the areas with reduced lateral diffusion may thus be a way by which cells control the apparent affinity of the ubiquitous ligand-reaction binding events.

This research was supported by INRIA grant “AE Co-Age” and a fellowship from Rhône-Alpes Region to B.C.

* hedi.soula@insa-lyon.fr

† hugues.berry@inria.fr

- [1] K. Jacobson, O. G. Mouritsen, and R. G. W. Anderson, *Nat Cell Biol* **9**, 7 (2007).
- [2] A. K. Kenworthy, B. J. Nichols, C. L. Remmert, G. M. Hendrix, M. Kumar, J. Zimmerberg, and J. Lippincott-Schwartz, *J Cell Biol* **165**, 735 (2004).
- [3] M. J. Schnitzer, *Phys Rev E* **48**, 2553 (1993).
- [4] M. Wachsmuth, W. Waldeck, and J. Langowski, *J Mol Biol* **298**, 677 (2000); I. M. Tolic-Norrelykke, E.-L. Munteanu, G. Thon, L. Oddershede, and K. Berg-Sørensen, *Phys Rev Lett* **93**, 078102 (2004); J.-H. Jeon, V. Tejedor, S. Burov, E. Barkai, C. Selhuber-Unkel, K. Berg-Sørensen, L. Oddershede, and R. Metzler, *ibid.* **106**, 048103 (2011).
- [5] I. Golding and E. C. Cox, *Phys Rev Lett* **96**, 098102 (2006).
- [6] M. Platani, I. Goldberg, A. I. Lamond, and J. R. Swedlow, *Nat Cell Biol* **4**, 502 (2002); I. Bronstein, Y. Israel, E. Kepten, S. Mai, Y. Shav-Tal, E. Barkai, and Y. Garini, *Phys Rev Lett* **103**, 018102 (2009).
- [7] J.-P. Bouchaud and A. Georges, *Phys Rep* **195**, 127 (1990).
- [8] R. Metzler and J. Klafter, *Phys Rep* **339**, 1 (2000).
- [9] M. J. Saxton, *Biophys. J.* **66**, 394 (1994); F. Höfling, T. Franosch, and E. Frey, *Phys Rev Lett* **96**, 165901 (2006).
- [10] M. Saxton, *J Chem Phys* **116**, 203-208 (2002); M. C. Bujan-Nunez and M. A. Lopez-Quintela, *ibid.* **121**, 886 (2004).
- [11] H. Berry, *Biophys J* **83**, 1891 (2002); M. Hellmann, D. W. Heermann, and M. Weiss, *Europhys Lett* **94**, 18002 (2011).
- [12] H. A. Soula, A. Coulon, and G. Beslon, *BMC Biophysics* **5**, 6 (2012).
- [13] Our diffusion algorithm corresponds to solving the Brownian motion with Ito’s stochastic calculus. Using Stratonovich’s rules preserves accumulation within the patch but with reduced intensity [3, 12].